Available online at www.sciencedirect.com
SCIENCE DIRECT®
Composites: Part A 35 (2004) 273-279
composites
Part A: applied science and manufacturing
www.elsevier.com/locate/compositesa

The compression of wood/thermoplastic fiber mats during consolidation

Karl R. Englund*, Michael P. Wolcott, John C. Hermanson

Wood Materials and Engineering Lab, Washington State Universiiy, Pullman, WA 99164-1806, USA

Received 22 July 2002; accepted 6 December 2002

Abstract

Secondary processing of non-woven wood and wood/thermoplastic fiber mats is generally performed using compression molding, where heated platens or dies form the final product. Although the study and use of wood–fibercomposites is widespread, few research efforts have explicitly described the fundamentals of mat consolidation. In contrast, the wood composite literature has prolifically addressed the compression of wood-strand composites. Models developed for wood-strand composites and powders are reviewed and applied to experimental data for compression of wood and wood/polypropylene (PP) fiber mats. The compression response was monitored during consolidation with varying platen temperatures, densities, and PP content. A model developed from the relationship between the instantaneous modulus and relative density was found to fit the compression of the non-woven fiber mats. The consolidation behavior was analogous to previous work with wood–fiber composites and found to be influenced by the PP content and strain rate.

Keywords: A. Wood; A. Fibres; E. Consolidation; Non-woven mats

1. Introduction

Non-woven mat technology uses both natural and synthetic fibers to produce a variety of interior use products. The fibrous mats provide the automotive industry with lightweight molded door panels, trunk liners, and dashboards, while other markets include residential door skins, cabinets, and furniture. Recent trends to improve the moisture resistance have included the addition of thermoplastic fibers to the mat network [1].

Non-woven mats are generally manufactured and sold to producers of auto or residential components. The mat integrity is maintained prior to secondary processing through friction among the interlocking wood and synthetic fibers. In some cases, thermoplastic resins are used as a preliminary adhesive to improve mat strength. A majority of the products manufactured with non-woven mats utilize thermal compression molding to form and maintain the final profile. Thermoset adhesives, such as phenol–formaldehyde (PF), are added to the mat to maintain panel integrity after pressing.

The consolidation mechanisms for wood-based composites have been researched by a variety of authors; Suchsland [2] and Jones [3], to name a few. Suchsland [2] noted that the stress–strain relationship of the mat is a function of the transverse cornpression of the wood. Jones [3] found the consolidation mechanism of a wood–fiber mat was not only a deformation of the wood fibers, but also due to fiber slippage and bending at contact points.

With the mechanisms of consolidation identified, models developed by Dai and Steiner [4], Wolcott et al. [5], Lang and Wolcott [6], and Lenth and Kamke [7] described the stress–strain behavior of a wood-strand mat. These models have been useful in identifying the contribution of different consolidation mechanisms in wood-strand composites. In turn, this work has been predicated on describing the formation and structure of the strand network. Unlike wood–fiber systems, void filling by strand shifting does not appear to play a role in strand mats. In addition, the fiber mats formed by blends of wood and thermoplastics differ from a wood-strand mat in both geometry and material type. Combined, these differences make strand-based models somewhat limited in their approach to model a fibrous mat. Therefore, alternative methods and disciplines are needed to describe the consolidation of a fibrous mat.

The powder research field has developed models that describe the stress–strain behavior of granulated materials.

* Corresponding author. Fax: +1-509-335-5077,
E-mail address: englund@mail.wsu.edu (K.R. Englund)

1359-835X/$ - see front matter © 2003 Elsevier Ltd. All rights reserved.
doi: 10.1016/j.compositesa.2002.12.001

Konopicky [8], Heckel [9], and Cooper and Eaton [10] established consolidation models for powders based on the relative density and void volume. As in wood–fiber mats, the mechanisms of powder consolidation rely on packing by void filling and particle deformation.

The goal of this research is to describe the stress developed during the compression of a non-woven wood and wood/polypropylene (PP) fiber mat. The specific objectives include: (1) provide a mathematical description of the compression response of a wood and blended wood/thermoplastic mat; (2) validate the model with laboratory consolidation experiments.

2. Mat compression

The development of a model for the compression of a wood/PP fiber mat must consider the response of the constitutive materials to an applied stress and the structure of the composite system. During consolidation, the mat densifies as the fibers reposition and deform. Therefore, developing a model to describe the stress behavior needs to address both fiber movement and deformation.

In an attempt to describe the compression response of a wood/thermoplastic fiber mat, models developed for consolidation of both wood-strand composites and powders are evaluated. Whereas studies addressing powder consolidation identifies volume or density ratio to be proportional to the applied compressive stress (s_c) [8–14], most of the models addressing consolidation of wood-strand mats utilize a Hookean relationship (Eq. (1)) modified with a non-linear strain function($y(e)$) [4,5,15,16].

$$\sigma_c = E_c \varepsilon \psi(\varepsilon) \tag{1}$$

where E_c is the compression modulus and e is the compressive strain.

Dai and Steiner [4] defined mat structure as a collection of independent strand columns of varying height, similar to the proposed model by Suchsland [2]. A Poisson's distribution was used to numerically describe the number of strands in localized strand columns. The probability ($p(i)$) of an infinitesimally small column containing i number of strands is given by a Poisson distribution (Eq. (2)). The maximum value of i, is based upon the thickness (z) of the wood element and the overall mat thickness. In the mat models, $p(i)$ equates to the fractional area of columns containing this number of strands within a mat.

$$p(i) = \frac{e^{-n} n^i}{i!} \tag{2}$$

The mean number of strands (n) is estimated for each discrete finite column and is calculated from the length (l) and width (w) of the strand, total number of strands allowed in one column, and the mat area (A). The total compressive stress of the composite during consolidation results from the sum of the discrete columns and can be estimated as:

$$\sigma_c = \sum_{i=1}^{i\,\max} \sigma_i = E_y \sum_{i=1}^{i\,\max} \psi(\varepsilon_i)\varepsilon_i p(i) \tag{3}$$

The terms s_i and e_i denote the stress and strain in columns with i number of strands and E_y is Young's modulus of the wood flake. The load resistance increases while the mat is compressed, increasing the total number of strand columns supporting the load. Dai and Steiner [4] neglect any stresses prior to column compression. Lang and Wolcott [6, 15] utilized beam theory to augment the column compression approach. Departing from a theoretical approach, Monte Carlo techniques were used to simulate mat structures obtained from measurements of digitized images of flakeboard mats. Lenth and Kamke [7, 16] viewed a wood-strand mat as a cellular solid and utilized cellular theory to describe the stress–strain behavior of a wood-strand mat.

Many of the compaction studies for powders examine the influence of relative density (r_R) on s_c. The r_R is a ratio of the density of the powder bed compacted to any given strain to the density of the solid powder particles and is equivalent to the relative density used in foam models. Konopicky [8] proposed the relationship (Eq. (4)) between s_c and r_R with metal powders as:

$$\ln\left[\frac{1}{1-\rho_R}\right] = m\sigma_c \tag{4}$$

where m is a constant.

Heckel [9] also examined the compaction of various metal powders with a modified version of Konopicky's [8] relationship (Eq. (5)). Tabil and Sokhansanj [12] incorporated Heckel's [9] method to describe the compression of alfalfa grinds with good agreement. The results of the preceding work fit the data quite well at higher pressures, however, they failed to recognize the initial non-linear response of the compression curve.

$$\frac{d\rho_R}{d\sigma_c} = m(1-\rho_R) \tag{5}$$

In an attempt to describe the compression data of a non-woven mat, both strand and powder compression models can be utilized with limited success. However, the concepts behind these models can be applied to develop a more descriptive behavior of a fibrous mat in compression.

3. Experimental procedures

3.1. Uniaxial compression testing

Wood fiber and wood/PP fiber mats were obtained commercially (Mats Inc.). The mats were made with mechanically refined aspen (genus *Populus*) wood fibers coated with 5% PF resin and needled with 0, 30, 40, and 50% thermoplastic fibers, by weight. An additional 5% of

polyolefin coated polyester fibers (Celbond®) were also blended with the mat. The mat was passed through an oven to melt the polyolefin sheath, which provided the mat with integrity during handling.

Square test specimens (63.5 × 63.5 mm²), were cut from the mats for uniaxial consolidation. The mats were compressed to densities of 961, 1041 and 1121 kg/m³ at platen temperatures of 170, 180 and 190 °C. These platen temperatures were chosen to prevent thermal degradation of the wood (<200 °C [19]) and to exceed the melt temperature (T_m) of the PP (» 162 °C).

A final thickness of 6.35 mm was targeted, therefore, mats were layered upon each other to obtain the final density. A servo-hydraulic universal test apparatus with heated aluminum platens was used to compress the non-woven mat at strain rates of 0.15 and 0.30 mm/mm s. A thermocouple was inserted in the center of the layered mats to monitor the core temperature.

3.2. Differential scanning calorimetry

Differential scanning calorimetry (DSC) was utilized to identify the thermal transitions associated with the fiber mat components. A sample of the uncompressed wood and wood/PP fiber mats were Wiley® milled and passed through a 40 mesh screen. Approximately 5 mg of the screened material was weighed to the nearest 0.1 mg and encapsulated in a hermetically sealed pan. Utilizing a ramp rate of 10 °C/min, the specimen was heated from 40 to 200 °C, while the heat flow of the sample was recorded.

4. Results and discussion

4.1. Compression model

The compression curves for a wood/PP fiber mat were modeled with the same approach as Dai and Steiner [4], Lenth and Kamke [16], and Lang and Wolcott [15]. In each case the high strains associated with the fibrous mat could not be accounted for by any of the traditional strand-based models.

Utilizing the approach by Dai and Steiner [4], the wood element was considered to be an average wood fiber or fiber bundle for aspen species. The elements were square in their cross-section and had a length of 0.13 mm. In Fig. 1, z for the strand elements were 250, 25, and 12.5 μm, to represent a fiber bundle, single, and half fiber, respectively. The E_y was set at 25 MPa and y(e) was represented as the 10th order polynomial function utilized by Dai and Steiner [4]. In all elemental sizes, the experimental data failed to be described by the model. The strain at which stress begins to accumulate in the wood–fiber mats is approximately 0.9, substantially greater than that predicted by any of the wood-strand models.

One of the underlying assumptions of a Poisson distribution is that the likelihood of an event to occur is independent and cannot influence any other event [18]. In reality, the structure of a randomly oriented mat has overlapping and intertwining wood elements. In this case, the finite columns that comprise the mat structure do not necessarily behave as independent elements. Fibers that share columns may influence the stress–strain relationship of the neighboring columns. This assumption was recognized by Dai and Steiner [4], but was not found to strongly influence wood-strand mats. The larger aspect ratios found with wood and synthetic fibers may play a larger role in stress distribution throughout the mat. In addition, the influence of fiber bending and repositioning may render a consolidation model utilizing a Poisson's distribution inadequate for a fibrous network.

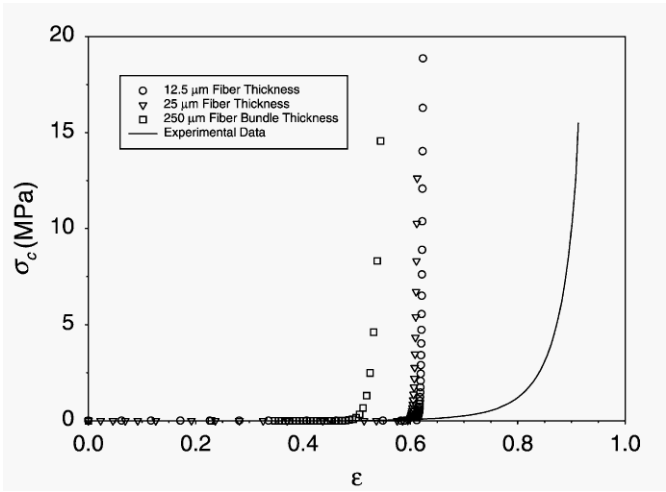

Fig. 1. Dai and Steiner's [4] compression model utilized with varying element cross-sectional dimensions. Compared to a non-woven mat with 0% PP compressed to a 1041 kg/m³ density at 180 °C.

The cellular model utilized by Lenth and Kamke [16] failed to fit their experimental data at the higher strains. The same was true for the wood/PP fiber mats in this study as an exponential increase in the data was observed at a lower strain of 0.65–0.75, depending upon the constants utilized in their cellular model. Lenth and Kamke [16] surmised their model did not consider the changing density of the cellular material, in this case, the wood strands. The same effect holds true for a wood/PP fiber mat. Similar results were also found when the experimental data was compared to the model developed by Lang and Wolcott [6]. The stress developed at the higher strains could not be accounted for in their model.

The poor prediction of strand mat consolidation models for wood/PP fiber mats is due to the large strains that occur during consolidation of fiber mats. In a loosely formed mat, a substantial amount of deformation occurs before stress begins to accumulate (Fig. 1). This would indicate a large amount of fiber movement, presumably through repositioning and bending. During fiber movement, voids are filled and the density continues to change until the cessation of strain. As the density increases, so do the mechanical properties of the composite. Mechanical testing of

the compressed wood composite exhibits a parabolic relationship between the density and modulus (E) of the composite [19]. Shivanand and Sprockel [11] found similar increases in tensile strength with highly compact cellulose powders.

Many of the powder compaction studies examine the influence relative density (r_R) has on s_c. However, the curve-fitting models utilized in the powder research did not address the low stress, non-linear region of the curve. This was also found to be true when the models of powder compression were utilized with the wood/PP fiber composites. The lack of fit with Konopicky [8] and Heckel's [9] models can be attributed to the linear relationship assumed between s_c and r_R. In powder compacts, this assumption of linearity can provide an accurate representation of the stress–strain response, however, with wood/PP fiber composites, the initial non-linear behavior of the compression curve is too substantial to overlook.

To describe the entire stress–strain behavior of a fibrous mat, instantaneous modulus $E(e)(ds_c/de)$ can be utilized. During the initial stages of consolidation, s_c is minimal and remains relatively constant due to fiber movement and rearrangement, which results in $E(e)$ approaching zero. However, as s_c increases non-linearly with e, during strains between 0.7 and 0.9, $E(e)$ begins to increase. Based upon the powder compaction literature [7], the following correlation between the change in modulus and relative density is postulated

$$\frac{dE(\varepsilon)}{E(\varepsilon)} = m\frac{d\rho_R}{\rho_R} \tag{6}$$

During consolidation, the r_R is related to strain (e) as

$$\rho_R = \frac{c}{1-\varepsilon} \tag{7}$$

$$d\rho_R = \frac{c}{(1-\varepsilon)^2}d\varepsilon \tag{8}$$

where c = initial r_R at $e = 0$.

Substituting Eqs. (7) and (8) into Eq. (6) yields the following proposed integral equation:

$$\int \frac{dE(\varepsilon)}{E(\varepsilon)} = m\int \frac{d\varepsilon}{1-\varepsilon} \tag{9}$$

Integrating Eq. (9) with respect to $E(e)$ and e, the natural logarithm of $E(e)$ becomes proportional to the compressive true strain (e_t) of the composite mat as seen in Fig. 2, which yields the following linear relationship:

$$\ln E(\varepsilon) = B + A\ln(1-\varepsilon) \quad \text{or} \quad E(\varepsilon) = (1-\varepsilon)^A e^B \tag{10}$$

where $\ln(1-e)$ = true compressive strain (e_t).

To determine s_c, $E(e)$ is defined as ds_c/de during consolidation. Separating the variables and taking the exponent of each side (Eq. (11)), yields A and B as coefficients of the linear approximation of $\ln E_t$ vs $\ln(e_t)$.

$$d\sigma_c = (1-\varepsilon)^A e^B d\varepsilon \tag{11}$$

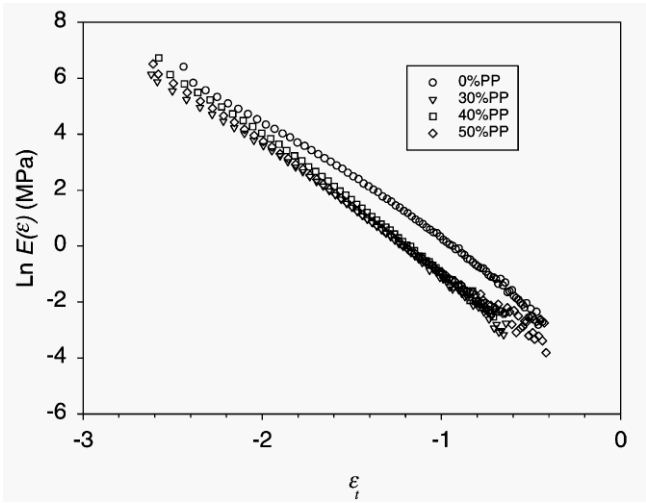

Fig. 2. Relationship between $E(e)$ and e_t for various percentage levels of PP at 180 °C platen temperature and 1041 kg/m³ density.

Integrating both sides with respect to s_c and e, the following estimate of the positive compressive stress is given by Eq. (12). A comparison of experimental data and the stress predicted in Eq. (12) is presented in Fig. 3. The average value of the coefficients A and B for varying PP content, density, and platen temperature at a 0.15 mm/mm s strain rate are provided in Table 1. The slope (A) of the relationship between $\ln(E(e))$ and e_t increases with increasing PP content. This corresponds to the similar behavior with the ultimate compressive stress, as the composite with PP required a higher stress to achieve the target density.

$$\sigma_c(\varepsilon) = -\frac{e^B}{(A+1)}[(1-\varepsilon)^{A+1} - 1] \tag{12}$$

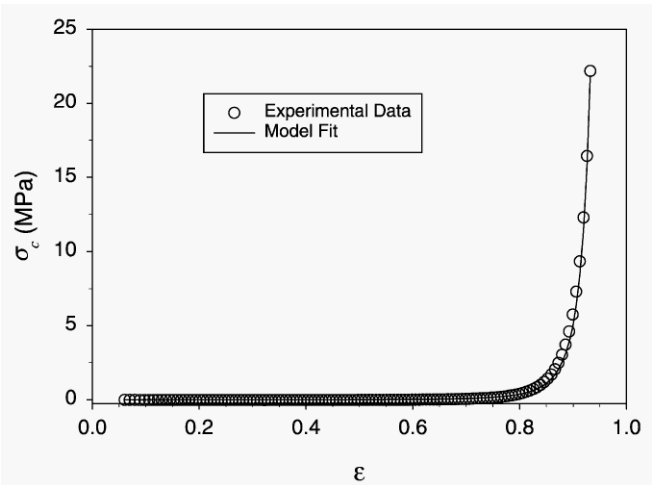

Fig. 3. Comparison of the modeled and experimental stress during the compression of a 50% PP wood–fiber mat at 180 °C and 1041 kg/m³ density.

Table 1
Linear coefficients, A and B for the $\ln(E(e))$ vs true strain plot, tested at a 0.15 mm/mm s strain rate

	Density (kg/m³)	0% PP		30% PP		40% PP		50% PP	
		A	*B*	*A*	*B*	*A*	*B*	*A*	*B*
170 °C	961	– 4.091	– 4.172	– 4.494	– 5.428	– 4.602	– 4.987	– 4.660	– 5.782
	1041	– 4.097	– 3.920	– 4.444	– 5.354	– 4.600	– 5.048	– 4.611	– 5.445
	1121	– 4.064	– 3.732	– 4.439	– 5.327	– 4.538	– 4.826	– 4.581	– 5.367
180 °C	961	– 4.094	– 3.966	– 4.456	– 5.509	– 4.739	– 5.530	– 4.712	– 5.904
	1041	– 4,069	– 3.789	– 4.456	– 5.254	– 4.664	– 5.321	– 4.718	– 5.694
	1121	– 4,074	– 3.886	– 4.398	– 5.270	– 4.615	– 5.089	– 4.571	– 5.380
190 °C	961	3.905	– 3.329	– 4.493	– 5.688	– 4.711	– 5.529	– 4.726	– 6.112
	1041	– 3.944	– 3.599	– 4.454	– 5.298	– 4.708	– 5.485	– 4.750	– 6.062
	1121	– 3.999	– 3.681	– 4.545	– 5.324	– 4.615	– 5.230	– 4.666	– 5.650

4.2. Compression behavior

The strain rate and PP content influenced the compression response of the wood/PP fiber mats. However, the platen temperature had little or no effect on the compressive stress behavior of the wood/PP mats (Fig. 4). Temperature can influence the mechanical properties of a polymer with the most substantial effect from glass and melt transitions. The lack of a temperature effect is likely due to the core temperatures remaining between ambient and 80°C during compression in all conditions. As evident in the DSC spectra for the 0 and 50% PP mats (Fig. 5), no thermal transitions occur within the major components of the composite between ambient and 80 °C. The melt transition exhibited in both curves at approximately 126 °C can be attributed to the polyolefin coated polyester fibers utilized in the non-woven mat process, while the PP melt at 163 °C can be seen in the 50% PP mat.

The change in strain rate was only found to influence the final compressive stress of the wood/PP mats, while little effect was seen in the 0% PP mats (Figs. 6 and 7). Suchsland [20] pressed wood particleboard with a range of strain rates and found a lower final compressive stress with the longer closing times. The strain rates used for the non-woven mats may have been too slow to see any time-dependent effects on the wood fibers. Also, the mechanical behavior of wood is not completely governed by viscoelasticity. The cellulose component is a highly crystalline material, which exhibits

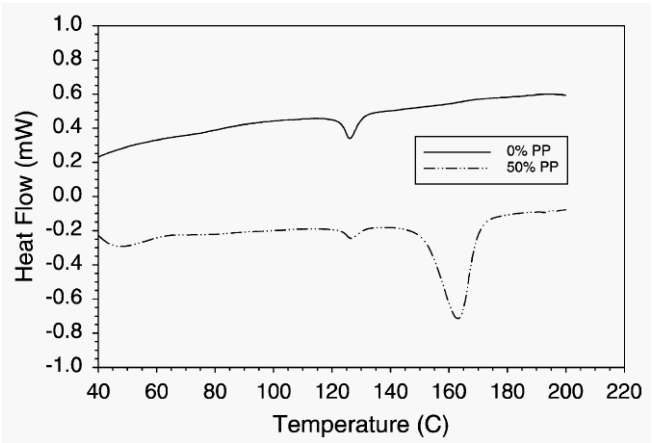

Fig. 5. DSC plot of 0 and 50% PP mats scanned at 10 °C/min using 40 mesh Wiley milled samples.

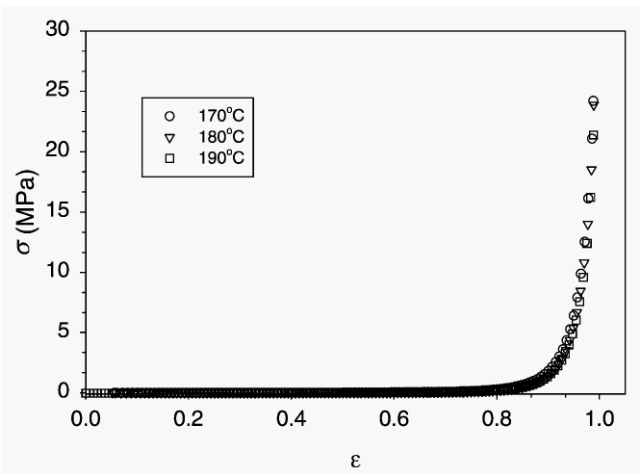

Fig. 4. Compression curve for non-woven mats with 40% PP pressed to 1041 kg/m³.

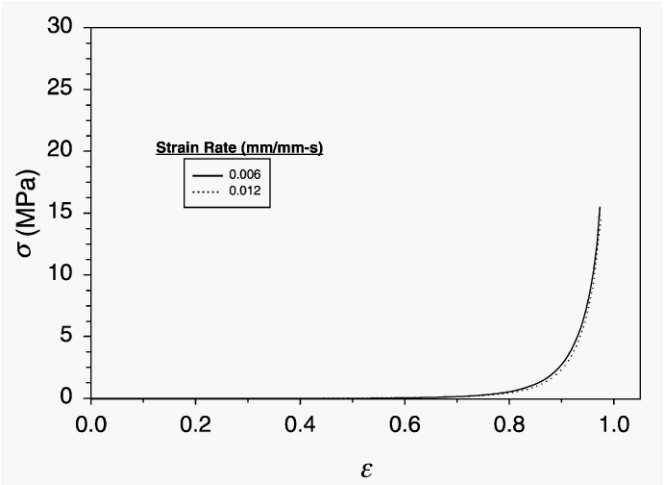

Fig. 6. Comparison of the compressive stress at varying strain rates for 0% PP mats pressed to a 1041 kg/m³ density at 180 °C.

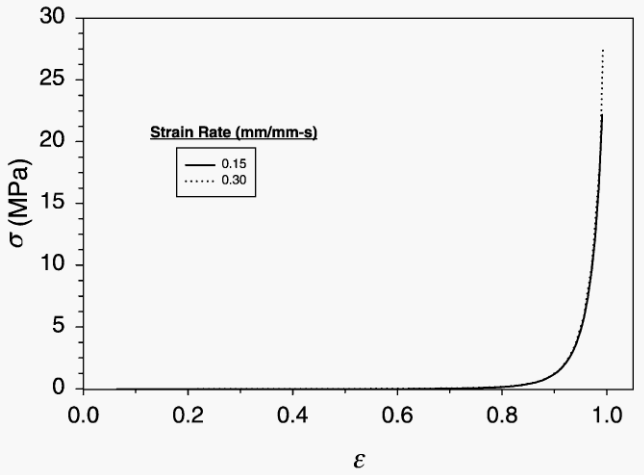

Fig. 7. Comparison of the compressive stress at varying strain rates for 50% PP mats pressed to a 1041 kg/m^3 density at 180 °C.

many elastic attributes [21]. The behavior of PP can be classified primarily as a viscoelastic material and would, therefore, be more susceptible to a time rate change than the mats with only wood fiber.

Jones [3] states that fiber bending and relocation dominate the initial stages of fiber mat compression. Dai and Steiner [4] and Lang and Wolcott [6] found the same conclusion for wood-strand composites. Since the bending modulus of wood is nearly four times higher than PP, the observation of Jones [3] holds true as the accumulation of stress occurs more quickly in the 0% PP mats (Fig. 8). Jones [3] also states the final stage of mat compression is dominated by fiber compression. Assuming a majority of the fibers lay within the plane of the platen, the properties of the fiber in the transverse direction would govern the stress behavior. The transverse compression modulus of aspen [22] is approximately one-tenth of PP, resulting in a lower final compressive stress for the high wood–fiber mats (Fig. 9).

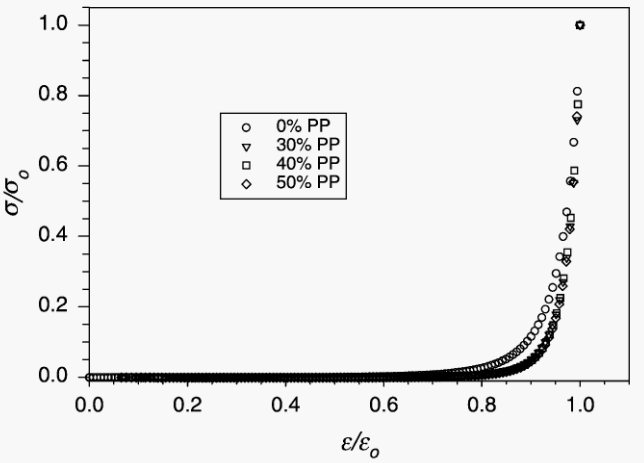

Fig. 8. Normalized compressive stress for varying PP levels pressed to 1041 kg/m^3 density with a platen temperature of 180 °C, where σ_0 and ε_0 are the ultimate compressive stress and strain, respectively.

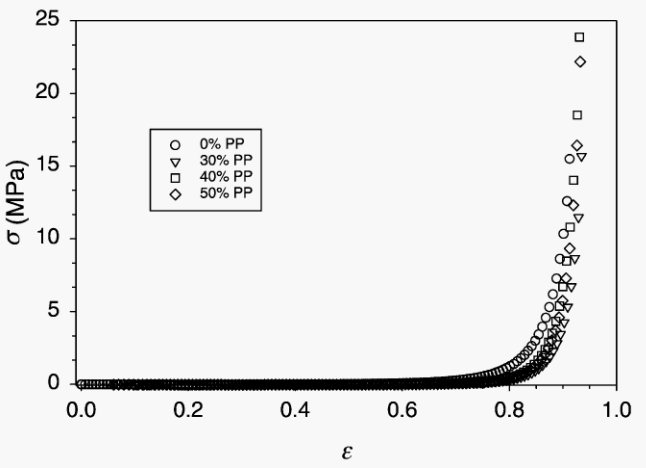

Fig. 9. Compressive stress for varying PP levels pressed to 1041 kg/m^3 density with a platen temperature of 180 °C.

5. Conclusion

When forming a wood and a wood/PP fiber composite through compression molding, heated platens apply stress to the mat until the final profile is established. The amount of stress required to compress the mat can depend upon the press closing speed or strain rate, platen temperature, and the composite formulation. Modeling the compressive stress with established methods in the wood-strand literature did not fit the experimental data. The lack of agreement results from the high strains developed in a wood–fiber mat and a disregard for the contribution of fiber bending and movement.

Following concepts used for consolidation of powders, a proportionality was postulated between the $E(\varepsilon)$ and ρ_R. Considering the change in ρ_R with ε was used to derive a new constitutive relation for fiber mats. The resulting non-linear relation could be easily fit experimental data with a high degree of accuracy. The two model parameters (A and B) were determined for a variety of mat compositions, platen temperatures, and final consolidation density.

The strain rate and PP content influenced the response of the stress–strain curve for the wood/PP mats. The addition of PP fibers increased the ultimate σ_c, while the mats with no PP exhibited a quicker accumulation of stress. Strain rate was found to influence the mats with PP fibers, but no rate effect was observed in the 0% PP mats. Differences in the observed platen temperatures did not appear to influence the consolidation behavior.

Acknowledgements

This research was funded by the USDA National Research Initiative Competitive Grants Program, Agreement No. 96355003804.

References

[1] Kryzysik AM, Youngquist JA, Myers GE, Chahyadi IS, Kolosick PC. Wood–polymer in extruded and nonwoven web composite panels. In: Proceedings of the Wood Adhesives Symposium; 1990. p. 183–9.

[2] Suchsland O. An analysis of the particleboard process. Michigan Q Bull 1959;42(2):350–72.

[3] Jones RL. The effect of fiber structural properties on compression response of fiber beds. Tappi 1963;46(1):20–7.

[4] Dai C, Steiner PR. Compression behavior of randomly formed wood flake mats. Wood Fiber Sci 1993;25(4):349–58.

[5] Wolcott MP, Kamke FA, Dillard DA. Fundamental aspects of wood deformation pertaining to manufacture of wood-based composites. Wood Fiber Sci 1994;26(4):496–511.

[6] Lang EM, Wolcott MP. A model for viscoelastic consolidation of wood-strand mats. Part 1. Structural characterization of the mat via monte carlo simulation. Wood Fiber Sci 1996;28(1):100–9.

[7] Lenth CA, Kamke FA. Investigations of flakeboard mat consolidation. Part I. Characterizing the cellular structure. Wood Fiber Sci 1996; 28(2):153–67.

[8] Konopicky K. In: Sintereisen and Sinteristabl. Wein: Springer; 1948.

[9] Heckel RW. An analysis of powder compaction phenomena. Trans Metall Soc AIME 1961;221:1001–8.

[10] Cooper AR, Eaton LE. Compaction behavior of several ceramic powders. J Am Ceram Soc 1962;45(3):97–101.

[11] Shivanand P, Sprockel OL. Compaction behavior of cellulose polymers. Powder Technol 1992;69:177–84.

[12] Tabil Jr LG, Sokhansanj S. Compression and compaction behavior of alfalfa grinds. Part 1: compression behavior. Powder Handling Process 1996;8(1):17–23.

[13] Helle AS, Easterling KE, Ashby MF. Hot-isotatic pressing diagrams: new developments. Acta Metall 1985;33(12):2163–74.

[14] Walker EE. The properties of powders. Part VI. The compressibility of powders. Trans Faraday Soc 1923;19:73–82.

[15] Lang EM, Wolcott MP. A model for viscoelastic consolidation of wood-strand mats. Part II. Static stress–strain behavior of the mat. Wood Fiber Sci 1996;28(3):369–79.

[16] Lenth CA, Kamke FA. Investigations of flakeboard mat consolidation. Part II. Modeling mat consolidation using theories of cellular materials. Wood Fiber Sci 1996;28(3):309–19.

[17] Goldstein IS. Degradation and protection of wood from thermal attack. In: Nicholas DD, editor. Wood deterioration and its prevention by preservative treatments, vol. 1. Degradation and protection of wood. New York: Syracuse University Press; 1973.

[18] Ang AH, Tang WH. Probability concepts in engineering planning and design. New York: Wiley; 1975.

[19] Wong ED, Zhang M, Wang Q, Kawai S. Formation of the density profile and its effects on the properties of particleboard. Wood Sci Technol 1999;33:327–40.

[20] Suchsland O. Behavior of a particleboard mat during the press cycle. Forest Products J 1967;17(2):51–7.

[21] Mark RE. Cell wall mechanics of tracheids. New Haven, CT: Yale University Press 1967.

[22] Bodig J, Goodman JR. Prediction of elastic parameters for wood. Wood Sci 1973;5(4):249–64.